



Stereochemical diversity of AI-2 analogs modulates quorum sensing in *Vibrio harveyi* and *Escherichia coli*

Fabio Rui^{a,b}, João C. Marques^{a,b,c}, Stephen T. Miller^d, Christopher D. Maycock^{a,e}, Karina B. Xavier^{a,b}, M. Rita Ventura^{a,*}

^a Instituto de Tecnologia Química e Biológica, Av. da República, Estação Agronómica Nacional, 2780-157 Oeiras, Portugal

^b Instituto Gulbenkian de Ciência, Rua da Quinta Grande 6, 2780-156 Oeiras, Portugal

^c Presently at Champalimaud Neuroscience Programme, Champalimaud Centre for the Unknown, Av. Brasília s/n, 1400-038 Lisboa, Portugal

^d Department of Chemistry and Biochemistry, Swarthmore College, Swarthmore, PA 19081, USA

^e Faculdade de Ciências da Universidade de Lisboa, Departamento de Química e Bioquímica, 1749-016 Lisboa, Portugal

ARTICLE INFO

Article history:

Received 13 August 2011

Revised 4 November 2011

Accepted 5 November 2011

Available online 12 November 2011

Keywords:

AI-2

DPD

DPD analogs

DPD agonist

Quorum sensing

ABSTRACT

Bacteria coordinate population-dependent behaviors such as virulence by intra- and inter-species communication (quorum sensing). Autoinducer-2 (AI-2) regulates inter-species quorum sensing. AI-2 derives from the spontaneous cyclisation of linear (*S*)-4,5-dihydroxypentanedione (DPD) into two isomeric forms in dynamic equilibrium. Different species of bacteria have different classes of AI-2 receptors (LsrB and LuxP) which bind to different cyclic forms. In the present work, DPD analogs with a new stereocenter at C-5 (4,5-dihydroxyhexanediones (DHDs)) have been synthesized and their biological activity tested in two bacteria. (4*S*,5*R*)-DHD is a synergistic agonist in *Escherichia coli* (which contains the LsrB receptor), while it is an agonist in *Vibrio harveyi* (LuxP), displaying the strongest agonistic activity reported so far ($EC_{50} = 0.65 \mu\text{M}$) in this organism. Thus, modification at C-5 opens the way to novel methods to manipulate quorum sensing as a method for controlling bacteria.

© 2011 Elsevier Ltd. All rights reserved.

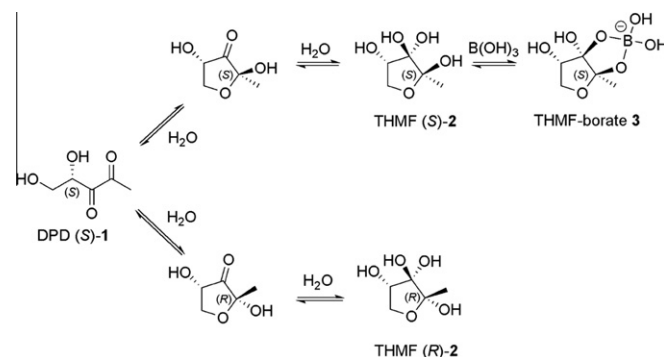
1. Introduction

Bacterial cells coordinate their behavior in order to adapt to environmental conditions. Cell-to-cell communication occurs through the secretion and sensing of substances called autoinducers. This process, known as quorum sensing, allows bacteria to synchronize behaviors according to the density of their population. Most autoinducers described so far are species-specific, however, one of them, autoinducer-2 (AI-2), is shared by many bacterial species,¹ allowing different species to influence each other's behavior.² Initially discovered in marine bacterium *Vibrio harveyi* where it induces bioluminescence,³ AI-2 is now known to regulate important processes such as biofilm formation, toxin production and virulence in a variety of species.^{4,5} Because AI-2 also regulates behaviors of human pathogens such as *Vibrio cholerae*,⁶ there is great interest in the discovery of non-natural quorum sensing modulators⁷ for applications in the treatment of bacterial infections.⁸

As illustrated in Scheme 1, the AI-2 signal derives from the spontaneous cyclisation of the linear (*S*)-4,5-dihydroxypentanedione (DPD) (*S*)-1 into isomeric forms which co-exist in a dynamic equilibrium. In water, the tetrahydroxytetrahydrofuran (THMF)

(*S*)-2 and THMF (*R*)-2 and the linear hydrated form of DPD coexist in a ratio of approximately 2:2:1; in presence of boron, borate complexes such as THMF-borate-3 are formed.⁹

A peculiarity of AI-2 signaling is that diverse bacteria have different AI-2 receptors which recognize distinct forms of AI-2. So far two AI-2 receptors have been identified: LuxP binds THMF-borate 3,¹⁰ while LsrB binds THMF (*R*)-2.¹¹ The crystal structures of



Scheme 1. Forms of AI-2 in water.

* Corresponding author.

E-mail address: rventura@itqb.unl.pt (M.R. Ventura).

the two ligand/receptor complexes showed that both proteins have very different binding sites,^{10,11} thus explaining why they accommodate different forms of AI-2.

The LsrB receptor was first identified in *Salmonella typhimurium*¹¹ and it is present in most enteric bacteria like *Escherichia coli* but also in more distantly related bacteria such as the plant symbiont *Sinorhizobium meliloti*¹² and the human pathogen *Bacillus anthracis*.¹³ In contrast, the LuxP receptor seems to be restricted to bacteria from the *Vibrio* genera.¹⁰

S. typhimurium, *E. coli* and *V. harveyi* are the best characterized bacteria in terms of AI-2 signaling, thus the activity of structural analogs of DPD has been tested in reporter strains of these species. So far, the design of bioactive analogs has focused on the replacement of methyl group at C-1 of DPD with linear,^{14–16} branched and cyclic^{17,18} alkyl groups, as well as with a trifluoromethyl substituent.¹⁹ Synthetic inhibitors based on an arylsulfonyl thioester scaffold were shown to be effective in *V. harveyi*,²⁰ and a brominated natural product was shown to inhibit different quorum sensing signals in this species.²¹ Among C-1 alkyl-DPD analogs, CF₃-DPD proved to be a weak agonist¹⁹ and hexyl-DPD was the only inhibitor reported in *V. harveyi*, with IC₅₀ of approximately 10 μM.¹⁵ Surprisingly, all C-1 alkyl-DPD analogs assayed in *V. harveyi* proved to be synergistic agonists in presence of physiological concentration of DPD, enhancing bioluminescence induced by the natural autoinducer.^{14,16,17} The same analogs were also tested in the enteric bacteria *S. typhimurium*¹⁴ and *E. coli*,¹⁸ but in these cases antagonistic activity towards AI-2 was observed. The most potent inhibitor reported for enteric bacteria is butyl-DPD with IC₅₀ of approximately 5 μM.¹⁴ Thus, these synthetic structural analogs of DPD reveal that minor alterations can have profound impact on their biological effects and that these effects differ depending on the class of AI-2 receptor tested.

Due to the tendency of the target products to rearrange and polymerize, the synthesis of DPD and its analogs is challenging,⁹

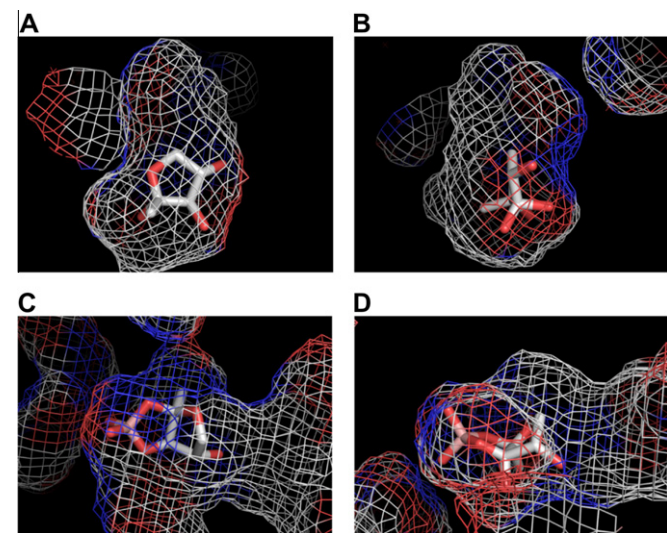
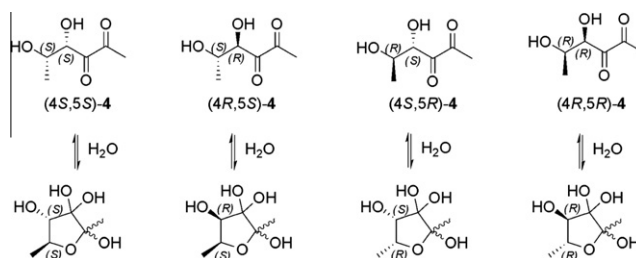


Figure 1. (a) Mesh representation of surface of binding site and (adjacent cavity) inside the *S. typhimurium* AI-2 receptor (LsrB; PDB ID 1TJY) as calculated by PyMOL.²³ Position of biological ligand (THMF (R)-2), as determined by X-ray crystallography, shown in stick representation. The same color scheme (oxygen = red, nitrogen = blue, carbon = white, boron = pink) is used for both. The colors of the mesh show the identity of the atom at the surface of the protein at that position: red and blue are hydrophilic regions (oxygen and nitrogen) and white hydrophobic (carbon) (b) As in (a), rotated 90 degrees about the y-axis. (c) Mesh representation of surface of binding site (and adjacent cavities) inside the *V. harveyi* AI-2 receptor (LuxP; PDB ID 1JX6) as calculated by PyMOL and position of the biological ligand (and THMF-borate 3), as determined by x-ray crystallography, shown in stick representation. (d) As in (c), rotated 90 degrees about the x-axis.



Scheme 2. Synthetic DPD analogs: 4,5-dihydroxyhexanediones **4** (DHDs).

thus, despite the promising results mentioned above, only C-1 and, more recently, carbocyclic structural analogs have been tested for their biological properties.^{14–19,22}

Here we explore the impact of the novel modification of DPD at C-5. Because the crystal structures of LsrB¹¹ and LuxP¹⁰ reveal a cavity in the binding sites of both receptors in proximity of the C-5 methylene group of the natural ligands (Fig. 1), substitution at this position should provide new leads for bioactive DPD analogs. Therefore enantiopure analogs of DPD modified in position C-5, that is, 4,5-dihydroxyhexanedione **4** (DHD) were prepared: (4S,5S)-**4**, (4R,5S)-**4**, (4S,5R)-**4** and (4R,5R)-**4** (Scheme 2). These compounds were tested for response from both LsrB and LuxP type receptors: in vivo with the *E. coli* reporter assay and with the more common *V. harveyi* in vivo assay and in vitro with an assay that directly measures binding to purified LuxP protein.

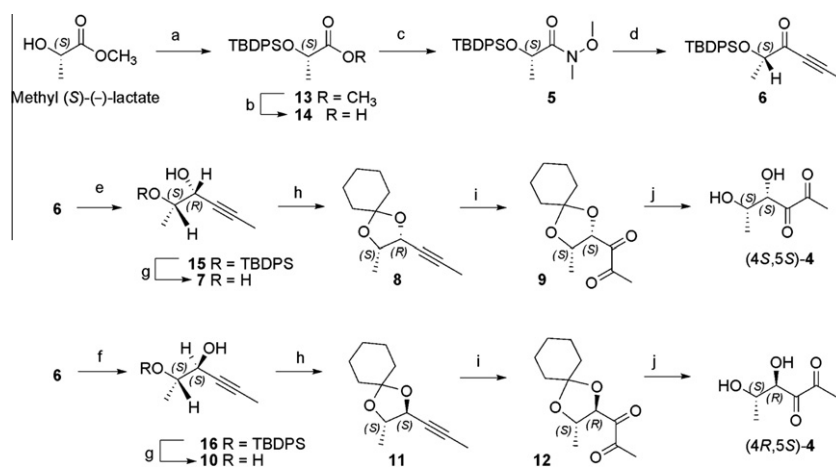
2. Results

2.1. Synthesis and structural characterization of the C-5-DPD analogs

Four diastereoisomers of 4,5-dihydroxyhexanedione **4** (DHD, Scheme 2) were prepared as enantiopure compounds starting from (S)- and (R)-methyl lactate.

As outlined in Scheme 3, methyl (S)-lactate was transformed into its *Weinreb* amide **5** in three steps, using an efficient method for the coupling of carboxylic acid with *N,O*-dimethylhydroxylamine.²⁴ This procedure improves our published synthesis of the DPD-scaffold from methyl glycolate,²⁵ because it provides *Weinreb* amide in high yield without chromatographic purification. Amide **5** was homologated to the silyloxyhexynone **6**, which was reduced with two different stereoselective methods. In the first one, addition of hydride from (S)-Alpine Borane[®] and deprotection provided diol **7** with high diastereoisomeric purity (*dr* = 0.95), as determined by NMR. Protection of the diol as cyclohexylidene-acetal **8** and subsequent oxidation, as described for the synthesis of DPD,⁹ provided intermediate **9**, which gave DHD (4S,5S)-**4** after acidic hydrolysis. In the second reduction method, ketone **6** was treated with Ce(III) and NaBH₄ in methanol at –50 °C;²⁶ subsequent fluorolysis resulted in diol **10** with high diastereoisomeric purity (*dr* = 0.95). After preparation of acetal **11** and of protected dihydroxydiketone **12**, acidic hydrolysis afforded (4R,5S)-**4**, the second of DHD diastereoisomers. Starting from methyl (R)-lactate through ketone *ent*-**6**, the same synthetic strategy described above resulted in (4R,5R)-**4**, using (R)-Alpineborane[®], and in (4S,5R)-**4**, using the inorganic reduction reagents.

The cyclohexanone released during hydrolysis was removed from the acidic solution washing quickly with chloroform; this byproduct does not inhibit bacterial growth in trace amount.⁹ Each stock solution of analog was quantified by ¹H NMR and used, as such, for the biological experiments. The amount of acid present did not significantly alter the pH of the buffer used for the experiments with bacteria and did not inhibit bacterial growth.



Scheme 3. Synthesis of two isomers of 4,5-dihydroxyhexanedione **4** (DHDs). Reagents and Conditions: (a) TBDPSCl, Et₃N, DMAP, CH₂Cl₂, 92%; (b) LiOH, THF/H₂O, quant. (c) CH₃(CH₃O)NH₂Cl, CDMT, NMM, THF, 84%; (d) propyne, BuLi, THF, -78 °C, 73%; (e) (S)-Alpine Borane, THF; (f) CeCl₃·7H₂O, NaBH₄, CH₃OH, -50 °C; (g) TBAF, THF, 36% **7** and 53% **10**, two steps, *dr* 0.95 for **7** and **10**; (h) *c*-hexanonedimethylacetal, H₂SO₄, DMF, 83%; (i) NaIO₄, cat. RuO₂·H₂O, CH₃CN/CCl₄/H₂O, 46%; (j) H₂SO₄ 0.01 M.

After peak assignment using COSY, HMBC and ¹H NMR, the distribution of linear and cyclic forms of DHDs in solution was monitored by ¹H NMR in D₂O. In the case of DPD the methyl group at C-1 is diagnostic because it results in two singlets at about 1.5 ppm when it is part of a hemiacetal in the two cyclic forms, while it gives a singlet at about 2.3 ppm when it is in the open-chain form.⁹ In the case of DHDs we observed only the signals of the C-1 methyl group in the cyclic forms at about 1.4 ppm in ¹H NMR (cf. Supplementary data S11 And S14, 1a and 1b), whereas the open-chain signal was detected only in the NOESY spectrum as an exchange peak with the cyclic forms (cf. S12 and S15, 'H1'). This shows that the cyclic, hydrated forms of DHD are essentially the only species to be found in solution (> 95%, cf. S11 and S14), the two anomers being present in roughly equal ratio. Therefore the introduction of a methyl group at C-5 of DPD alters the equilibrium distribution of linear and cyclic structures with respect to genuine DPD.⁹ The alkyl substituent α to the cyclizing heteroatom could favor ring formation due to a conformational effect (Thorpe-Ingold effect)²⁷ by analogy to the cyclization of γ-methyl-γ-butyrolactones.²⁸ The presence of exchange signals of the C-1 protons in NOESY (cf. S12 and S15, 'H1') experiments confirms the rapid interconversion between cyclic and open chain forms of DHD. Maintaining the fast equilibrium between the linear and cyclic forms is important for biological activity. Enteric bacteria recognize one cyclic form of DPD, but, once transported into the cytoplasm the open-chain form is phosphorylated and becomes active inside the cell.²⁹ Furthermore, locked cyclic analogs are impaired for biological activity both in *S. typhimurium* and *V. harvey*.²² As mentioned above our NOESY results show that the analogs prepared retain the requisite of equilibrium between open-chain and cyclic forms and thus are appropriate for the study of the biological effects of the additional stereogenic center at C-5 of DPD and its enantiomer.

2.2. Biological activity of DHDs in *E. coli*—a bacterium with the LsrB receptor

We used an *E. coli* reporter strain to evaluate the activities of the synthesized analogs in bacteria with the LsrB receptor. This assay uses a non-pathogenic strain instead of the more common *S. typhimurium* reporter strain for assaying the response of AI-2 and analogs in enteric bacteria.^{25,18} This *E. coli* strain, which carries a *lsr-lacZ* promoter fusion allows monitoring of the expression of *lsr*, the promoter induced by AI-2 in enteric bacteria, through the measurement of the β-galactosidase activity of cell extracts.^{30,31}

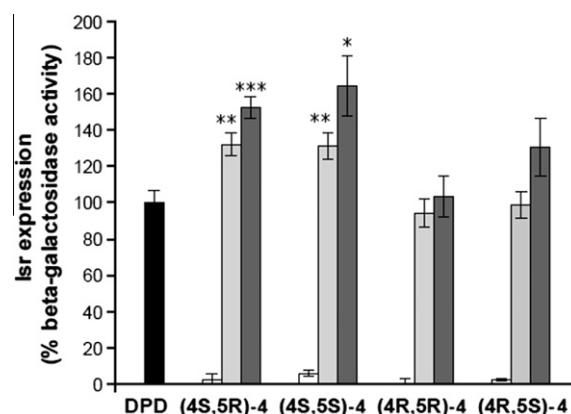


Figure 2. Synergistic effect of DPD and C5-DPD analogs in *E. coli*. Reporter strain KX1446 was incubated with DPD only (black bars, 20 μM); with analogs only (white bars, 150 μM); and with mixtures containing DPD (20 μM) and analogs (pale grey bars, 15 μM; dark grey bars 150 μM). Error bars indicate standard deviations; analysis of variance was performed with the Student's *t*-test.

As illustrated in Fig. 2, DHDs do not induce expression of the *lsr* genes if tested alone (agonist assay). However, in presence of the natural signal DPD (the typical antagonist assay), the analogs (4S,5R)-**4** and (4S,5S)-**4** are not antagonists but rather induce a significant increase in *lsr* expression over DPD alone. In contrast, the analogs with non-natural (4R)-configuration, (4R,5S)-**4** and (4R,5R)-**4**, do not show significant induction under the same conditions. Therefore the (4S,5R)-**4** and (4S,5S)-**4** are synergistic agonists of AI-2 in *E. coli*. This is an interesting difference from C-1 alkyl analogs of DPD, which have been shown to have a synergistic effect in *V. harvey*^{14,17} but not in bacteria with the LsrB receptor such as *E. coli*.

2.3. Biological activity of DHDs in *V. harvey*—a bacterium with the LuxP receptor

The same analogs were tested on the *V. harvey* system. Their effect was assayed both by means of a protein biosensor derived from the LuxP receptor³² and by measuring the bioluminescence of a *V. harvey* reporter strain.¹¹ The activities of the DHDs as assayed via the engineered LuxP receptor (CFP-LuxP-YFP) are shown in Fig. 3.

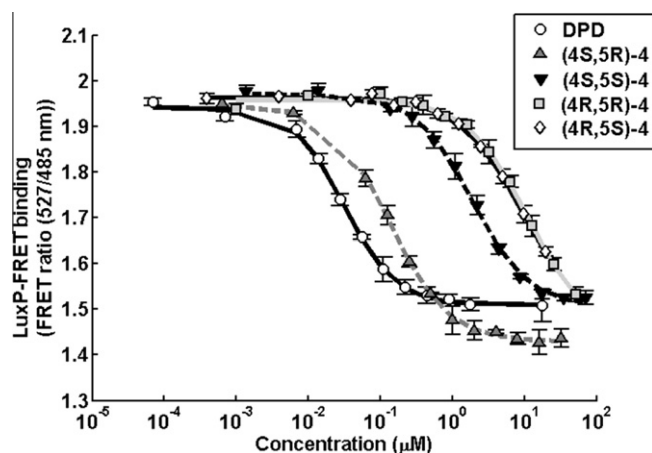


Figure 3. LuxP-FRET assay of DPD and C-5-DPD analogs. Error bars indicate standard deviations.

Binding of AI-2 to this engineered receptor causes a conformational change in the protein structure and a dose-dependent decrease in the fluorescence resonance energy transfer (FRET). Therefore a lower FRET ratio corresponds to an increase in ligand binding to LuxP.³² All the DHDs analogs induce a dose-dependent change in FRET ratio (Fig. 3), meaning that they all bind to the receptor. However, the EC₅₀ values (Table 1) indicate that they have very different affinities.

Small structural differences dramatically affect the interaction with the receptor protein. As expected, the natural (4S)-configuration results in the most active isomers (4S,5R)-4 and (4S,5S)-4. In addition, the (5R)-compound is more active than the (5S)-, meaning that the configuration at C-5 affects the interaction with LuxP.

The same pattern was observed *in vivo* using the *V. harveyi* reporter strain MM32, which is capable of inducing bioluminescence in an AI-2 dependent manner via the LuxP receptor.¹¹ As shown in Fig. 4, all analogs induce bioluminescence in the absence of DPD (agonist assay). However, in comparison with DPD, higher concentrations of DHDs are necessary to reach maximum induction and none of the analogues can induce the same levels of bioluminescence as DPD. This indicates that all DHDs are partial agonists of DPD.³³ In this *in vivo* assay, the configuration of the DHDs influences their activity in the same way as in the LuxP-FRET protein assay: the strongest agonist is (4S,5R)-4, while its (4S,5S)-isomer requires ten-fold higher concentrations to elicit the same response. The EC₅₀ for each compound is reported in Table 2.

As in the case of DPD, bioluminescence decreases at high concentrations of any of the analogs (Fig. 4). To test if there was an antagonistic effect of DHDs in competition with DPD, the same assay was performed in presence of the genuine signal (Supplementary data, Fig. S1).

Under these conditions, high concentrations of the isomeric DHDs reduce bioluminescence, suppressing the effect of DPD. The IC₅₀ were determined and, as shown in Table 2, the (4S,5S)-4 analog behaves as the strongest antagonist. Growth inhibition is observed at a concentration of 0.1 mM for all the compounds tested, but the inhibition is similar for DHDs and DPD (Supplementary data Fig. S2) and thus the antagonistic effect cannot be ascribed to toxicity. Overall, this suggests that in these conditions the DHDs compete with DPD for LuxP binding.

The results obtained with *V. harveyi* show that DHDs mimic DPD: they behave as partial agonists in the sub-micromolar to low-micromolar concentration range, and they have antagonistic effects at higher concentrations. Agonistic activity shows a clear structure-activity relationship trend, the (5R)-configuration being more active than the (5S).

Table 1

Binding affinity of C-5 DPD analogs to CFP-LuxP-YFP by the LuxP-FRET assay

Compound	EC ₅₀ in LuxP-FRET assay (μM) ^a
DPD	0.032 ± 0.0015
(4S,5R)-4	0.14 ± 0.019
(4S,5S)-4	1.87 ± 0.22
(4R,5R)-4	11.6 ± 2.8
(4R,5S)-4	10.0 ± 2.4

^a Assay performed with varying concentrations of test compound. Values obtained from data in Fig. 3.

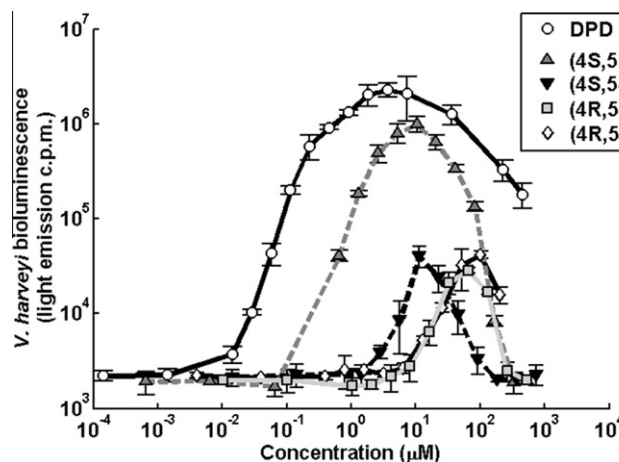


Figure 4. Bioluminescence assay of DPD and C-5 DPD with *V. harveyi* reporter strain MM32. Error bars indicate standard deviations.

Table 2

Summary of quorum sensing modulation by DPD and C-5 DPD analogs in *V. harveyi*

Compound	EC ₅₀ ^a (μM)	IC ₅₀ ^b (μM)
DPD	0.076 ± 0.002	—
(4S,5R)-4	0.65 ± 0.05	169 ± 19
(4S,5S)-4	6.21 ± 0.46	57.54 ± 0.29
(4R,5R)-4	19.5 ± 6.3	159.7 ± 8.4
(4R,5S)-4	26.5 ± 8.4	— ^c

^a Assay performed with varying concentrations of test compound, values obtained from the data in Fig. 4.

^b Assay performed with varying concentrations of test compound in the presence of 0.1 μM of DPD; values obtained from the data in Supplementary Fig. S1.

^c Not determined.

As shown in Table 2, the analog (4S,5R)-4 has an EC₅₀ of 0.65 μM. This is the strongest DPD agonistic activity among known analogs. The most potent synthetic agonists of AI-2 reported so far, CF₃-DPD and the opposite enantiomer of DPD, (R)-1, have EC₅₀ ranging between 30 and 84 μM.^{19,34} DHDs show independent agonistic activity and thus have a different biological effect than C-1 alkylated analogs of DPD which, with the exception of hexyl-DPD and CF₃-DPD, are generally active only in presence of DPD in *V. harveyi*.^{14,16,17}

3. Discussion

The introduction of a new stereocenter at C-5 of the DPD scaffold resulted in four diastereoisomeric analogs, DHDs, with interesting biological effects. The analogs were tested in model bacteria that recognize AI-2 via either the LsrB or the LuxP receptor. The response for the (4R)-DHD isomers was weak in both systems. In contrast, a synergistic response to (4S)-DHD isomers in the presence of DPD was observed in *E. coli*, whereas (4S,5R)-DHD showed a agonistic response stronger than (4S,5S)-DHD in

V. harveyi. The weak induction observed in both systems by the (4*R*)-DHDs was not surprising because similar responses had been reported for (4*R*)-DPD. Thus, these results reinforce the importance of the (4*S*)-configuration for AI-2 dependent response in the two systems tested.

In the AI-2 based induction of the *V. harveyi* quorum sensing system, the known receptor is LuxP and there is no evidence for another protein involved in AI-2 recognition. In contrast, the *E. coli* response to AI-2 is more complex. Induction of AI-2-dependent *lsr* activation requires that cyclic THMF (*R*)-**2** bound to LsrB is transported to the cytoplasm and then that the open-chain form is phosphorylated at the C-5 hydroxyl group by the kinase LsrK. This phosphorylated AI-2 then deactivates the repressor of the AI-2 response (LsrR). It is known that LsrB is not essential for *E. coli* AI-2 response, but activation is clearly stronger when the receptor is present.³¹ In addition, a recent report showed that the kinase is not very selective and can phosphorylate a broad range of DPD analogs as long as the hydroxyl group at C-5 is maintained,¹⁸ which is the case for the DHDs. The observed synergistic effect in *E. coli* is interesting, but, as with the C1-analogs in *V. harveyi*,^{14,16,17} a molecular explanation for the effect is still lacking and further work is required.

Within the two signaling system tested, there is a notable distinction in the response of the different species to the (4*S*,5*R*)-DHD and (4*S*,5*S*)-DHD diastereoisomers. Specifically, *E. coli* (LsrB receptor) react similarly to both enantiomers, while *V. harveyi* (LuxP) responds more strongly to (4*S*,5*R*)-DHD, suggesting better binding of this ligand to the LuxP receptor. This behavior can be rationalized through analysis of the crystal structures of the receptors with their natural ligands. Both receptors are two domain proteins with the ligand binding site located between the domains, adjacent to a hinge region that connects the domains.^{9–11} As shown in Fig. 1 (panels A and B), the C-5 carbon of (*R*)-THMF-**2** is oriented away from the surface of the LsrB binding site, towards an unfilled region. Visual analysis suggests that there would be no significant difference in steric interaction with the protein between the 5*R* and 5*S* isomers, in agreement with our experimental data showing similar *E. coli* response to both DHDs. On the other hand, *V. harveyi* (LuxP) does show stereospecific dependence, with a 10-fold stronger response to (4*S*,5*R*)-DHD than to (4*S*,5*S*)-DHD. As shown in Figure 1 (panels C and D), a 5*S* methyl would be oriented toward (and, presumably, come into steric conflict with) the protein while the 5*R* form would position the extra methyl on the face of the ring nearer the large cavity in the binding site. Some conformational change in the protein and/or ligand is expected when LuxP binds a DHD rather than the biological ligand; the space provided by the cavity should facilitate such changes. Moreover, the region of the protein near the position presumed to be occupied by a 5(*R*) methyl is largely hydrophobic (white in Fig. 1C and D), suggesting both a favorable protein/ligand interaction and that fewer hydrogen bonds would be broken in any minor conformational changes induced by binding of (4*S*,5*R*)-DHD as opposed to (4*S*,5*S*)-DHD. Thus, relative proximity of the 5(*R*) methyl to the binding site cavity provides a reasonable explanation for the observed stronger response of *V. harveyi* to (4*S*,5*R*)-DHD.

4. Conclusions

The four stereoisomers of 4,5-dihydroxyhexanedione (**4**, DHD) have been prepared starting from the enantiomeric methyl lactates of high optical purity. These new analogs of DPD are the first AI-2 synergistic agonists reported so far in enteric bacteria. In the alternative signaling system *V. harveyi*, DHDs having (5*R*)-configuration have increased agonistic activity compared to the (5*S*)-configuration. In particular, the analog (4*S*,5*R*)-**4** is the strongest AI-2 agonist described so far in *V. harveyi*, with

$EC_{50} = 0.65 \mu\text{M}$. Based on the analysis of the crystal structures available for LsrB and LuxP bound to their natural ligands, we propose an explanation that supports the experimental data obtained with the different analogs tested. Knowledge of the biological activity of C-5 substituted DPD analogs complements that of the known C-1 alkyl analogs and should be useful for the design of novel quorum sensing modulators.

5. Experimental

5.1. Synthesis

All solvents were distilled prior to use. The optical purity of the starting materials purchased was ee = 97% for methyl (*S*)-lactate and ee = 96% for methyl (*R*)-lactate (GLC, supplier specifications). The following abbreviations are used in the text: Hex, hexanes; EA, ethyl acetate, Et₂O, diethyl ether, MeOH, methanol; AcOH, acetic acid. Dry THF was distilled from sodium, dry CH₂Cl₂ was distilled from P₂O₅. Pooled organic phases were dried on MgSO₄. ¹H NMR spectra were recorded in CDCl₃ at 400 MHz, using TMS as internal standard or 3-(trimethylsilyl)-propanesulfonic acid in D₂O. *J* values are given in Hz. ¹³C NMR spectra were recorded at 100 MHz, using the solvent peak as internal standard in CDCl₃. Peak assignment was based on correlation experiments (HMQC, HMBC, ¹H, ¹H COSY). D₂O used for NMR contained 1% of 1 M H₂SO₄ solution in H₂O. TLC was performed on aluminium sheets coated with Kieselgel 60 F₂₅₄. Flash column chromatography was carried out on silica 60 μm; Medium Pressure Liquid Chromatography was performed on 45–60 μm silica. Specific rotations were measured using a 1 dm path length thermostated cell, values between –2 and +2 could not be measured with sufficient precision and are not reported. HRMS were measured either by ESI-TOF-MS with Flow Injection Analysis or by DIP-EL-MS.

5.1.1. Preparation of (2*S*)-2-*t*-butyldiphenylsilyloxypropanoic acid methyl ester (**13**) or *ent*-**13**

A solution of *tert*-butyldiphenylchlorosilyl (3.02 g, 11 mmol) in CH₂Cl₂ (3 ml) was slowly added to a solution containing methyl (*S*)-lactate (1.04 g, 10 mmol), TEA (1.09 g, 1.5 ml, 11 mmol) and DMAP (50 mg, 0.04 equiv) in dry CH₂Cl₂ (2 ml). After 15 h the suspension was treated with saturated NH₄Cl (5 ml) and extracted with CH₂Cl₂ (3 × 20 ml). The organic phases were washed with NH₄Cl, dried and evaporated. Purification on column chromatography (Hex/EA 95:5) gave a colorless liquid (3.15 g, 92%). [α]_D²⁰ –44.4 (c 1.20; CH₂Cl₂). The same procedure applied to methyl (*R*)-lactate gave product *ent*-**13** [α]_D²⁰ +45.7 (c 0.95 in CH₂Cl₂). ¹H NMR, ¹³C NMR and IR spectra matched literature data.³⁵

5.1.2. Preparation of (2*S*)-2-*t*-butyldiphenylsilyloxypropanoic acid (**14**) or *ent*-**14**

Ester **13** (3.08 g, 9.0 mmol) was dissolved in THF (9 ml) in a 100 ml beaker, and an aqueous solution of LiOH (0.6 M, 47 ml, 28 mmol) was added. The mixture was covered and stirred at 1000 rpm with a stirring bar sweeping the full internal diameter of the beaker. After 2 h, solid LiOH (648 mg, 27 mmol, 3 equiv) was added and, after additional 16 h, hydrolysis was complete (TLC, Hex/EA 9:1 + 5% AcOH). The mixture was diluted with 5 ml of ether, acidified to pH 2–3 with 2 M HCl and extracted with ether (5 × 10 ml). The organic phases were pooled, dried and evaporated under reduced pressure, giving a colorless oil (2.95 g, quant.). ¹H NMR (CDCl₃, δ): 7.70–7.60 (m, 4H) and 7.50–7.35 (m, 6H); aromatics, 4.33 (q, *J* = 6.8 Hz, 1H, 6-H), 1.31 (d, *J* = 6.8 Hz, 3H, 3-H); 1.11 (s, 9H, C(CH₃)₃). ¹³C NMR (CDCl₃, APT, δ): 175.1 (–, C-1); 135.7 (+), 135.6 (+), 132.5 (–), 131.8 (–), 130.4 (+), 130.3 (+), 128.0 (+), 127.9 (+); aromatics; 69.4 (+, C-2); 26.9 (+, C(CH₃)₃); 20.9

(+, C-3); 19.1 (–, C(CH₃)₃). IR (film, cm⁻¹): br 3500–3000, 3072, 3051, 2956, 2933, 2859, 1724 (C=O). [α]_D²⁰ –9.4 (c 1.00 in CH₂Cl₂). The same procedure applied to ester **ent-13** gave acid **ent-14**; [α]_D²⁰ +9.9 (c 0.95 in CH₂Cl₂).

5.1.3. Preparation of (2S)-N-methoxy-N-methyl-2-(*t*-butyldiphenylsilyloxy)propanamide (**5**) or **ent-5**

2-Chloro-4,6-dimethoxy-[1,3,5]-triazine (1.85 g, 10.6 mmol, 1.2 equiv) and *N*-methylmorpholine (2.9 mL, 26.4 mmol, 3 equiv) were added to a solution of **14** (2.9 g, 8.8 mmol) in THF (26 ml) stirred under Ar atmosphere. After stirring the mixture for 45 min, solid *N,O*-dimethyl-hydroxylamine hydrochloride (0.86 g, 8.8 mmol, 1 equiv) was added. After 5 h and TLC control (H/EA 7:3) the reaction was quenched with water (39 ml) and the mixture extracted with Et₂O (3 × 20 ml). The pooled organic phases were washed twice with sat. Na₂CO₃, 1 M HCl and brine, then dried and concentrated at reduced pressure. The dense liquid obtained was filtered through a pad of silica eluted with H/EA 7/3. The filtrate crystallized at room temperature (2.75 g, 84%). [α]_D²⁰ –15.4 (c 0.80 in CH₂Cl₂); mp: 64.9–65.8 °C. The same procedure was applied to acid **ent-14** resulting in amide **ent-5**. [α]_D²⁰ +14.7 (c 0.84 in CH₂Cl₂); literature³⁶ [α]_D²⁵ +12.1 (c 1.4 in CHCl₃); ¹H NMR, ¹³C NMR and IR spectra matched literature data.³⁶

5.1.4. Preparation of (2S)-2-*t*-butyldiphenylsilyloxyhex-4-yn-3-one (**6**) or **ent-6**

A 1.6 M solution of BuLi in hexane (6.2 ml, 10.0 mmol, 1.4 equiv) was added dropwise to a 1 M solution of propyne in THF (10.7 ml, 10.7 mmol, 1.5 eq.) cooled to –78 °C and stirred under Ar. The mixture was stirred for 30 min, and the temperature allowed to rise to 0 °C over 30 min and cooled again to –78 °C. A solution of amide **5** (2.65 g, 7.1 mmol) in THF (10 ml) was added dropwise and the suspension was slowly warmed to –20 °C and stirred for 1 h at this temperature. After TLC control (Hex/EA 7/3), sat. NH₄Cl solution (20 ml) was added, and the mixture acidified to pH 4 with 2 M HCl. The organic layer was separated and the aqueous solution was extracted with ether (3 × 20 ml). The pooled organic phases were washed with brine (2 ml), dried and evaporated at reduced pressure. Purification with MPLC (Hex/EA 9/1) gave a colorless oil (1.86 g, 73%). ¹H NMR (CDCl₃, δ): 7.75–7.65 (m, 4H) and 7.45–7.35 (m, 6H): aromatics; 4.23 (q, *J* = 6.8 Hz, 1H, H-2); 1.99 (s, 3H, H-6) 1.29 (d, *J* = 6.8 Hz, 3H, H-1); 1.11 (s, 9H, C(CH₃)₃). ¹³C NMR (CDCl₃, APT, δ): 189.8 (–, C-3); 135.8 (+), 133.6 (–), 133.0 (–), 129.8 (+), 127.6 (+): aromatics; 93.9 (–, C-4) 78.6 (–, C-5); 75.5 (+, C-2); 26.8 (+, C(CH₃)₃); 20.5 (+, C-1); 19.3 (–, C(CH₃)₃); 4.3 (+, C-6). IR (film, cm⁻¹): 3072, 3051; 2958; 2933; 2893; 2858; 2216 (C≡C); 1678 (C=O). HRMS (ESI-MS) calcd for C₂₂H₂₆NaO₂Si [M+Na]⁺ 373.1594, found 373.1583. [α]_D²⁰ –35.8 (c 0.80 in CH₂Cl₂). The same procedure applied to amide **ent-5** resulted in ketone **ent-6**; [α]_D²⁰ +35.8 (c 0.71 in CH₂Cl₂).

5.1.5. Preparation of (2S,3R)-hex-4-yn-2,3-diol (**7**) or **ent-7**

A 0.5 M THF solution of (*S*)-alpine borane (12.0 ml, 6.0 mmol) was added to a solution of ketone **6** (1.05 g, 3.0 mmol) in THF (1 ml) stirred under Ar. After 36 h, the starting material was not detected (TLC, Hex/EA 9/1); the reaction was quenched with a sat. solution of NH₄Cl (5 ml), and the mixture was extracted with CH₂Cl₂. After drying and evaporation of the organic phases, the residue was purified on MPLC (Hex/EA/MeOH 97/2/1) and analysed by NMR: ¹H NMR (CDCl₃, δ): 7.75–7.65 (m, 4H) and 7.5–7.35 (m, 6H): aromatics; 4.30–4.25 (m, 1H, C-3); 3.98–3.90 (m, 1H, C-2); 1.822 (d, 2.0 Hz, 3H, C-6); 1.13 (d, 6.4 Hz, C-1), 1.07 (s, 9H). The resulting material, containing semiprotected diol **15** and isomers with migrated silylether group, was not purified further. It was dissolved in THF (1 ml) under Ar and treated with a 1 M solution of TBAF in THF (1.6 ml, 1.6 mmol). After 5 h and TLC control (Hex/EA 6/4)

the reaction was quenched with sat. NH₄Cl (2 ml). The aqueous phase was saturated with solid NaCl and extracted exhaustively with EA (5 × 5 ml). Purification by gravity chromatography using flash silica (1st column Hex/EA 7/3 followed by pure EA; 2nd column Hex/EA 6/4) afforded **7** as a dense oil which solidified in the form of white flakes (124 mg, 36% over two steps). ¹H NMR (CDCl₃, δ): 4.30–4.22 (m, 1H, H-3); 3.89–3.80 (m, 1H, H-2); 2.20 (d, *J* = 7.0 Hz, 1H, –OH); 1.92 (d, *J* = 6.8 Hz, 1H, –OH); 1.883 (d, *J* = 2.1 Hz, 3H, H-6); 1.260 (d, *J* = 6.4 Hz, 3H, H-1). ¹³C (CDCl₃, APT, δ): 83.4 (–, C-4); 76.5 (–, C-5); 70.4 (+, C-2); 67.4 (+, C-3); 18.3 (+, C-1); 3.6 (+, C-6). IR (KBr, cm⁻¹) br 3600–3000: –OH; 2991; 2978; 2913; 2298; 2237 (C≡C). HRMS (ESI-MS): calcd for C₆H₁₀NaO₂ [M+Na]⁺ 137.0578, found 137.0557. [α]_D²⁰ –4.6 (c 0.74 in CHCl₃); *dr* = 0.95 (¹H NMR). The same procedure starting from ketone **ent-6** using (*R*)-alpine borane gave diol **ent-7**; [α]_D²⁰ +5.5 (c 0.80 in CHCl₃), *dr* = 0.95 (¹H NMR).

5.1.6. Preparation of (2S,3R)-2,3-(cyclohexylidenedioxy)-hex-4-yne (**8**) or **ent-8**

DMF (1 ml) in a small flask in an ice bath was acidified with one drop of conc. H₂SO₄ and an aliquot was diluted 1–10. Cyclohexanone dimethyl acetal (79 mg, 1.2 equiv) was dissolved in the diluted acidic DMF and this was added to diol **7** (52 mg, 0.46 mmol) in a 5 ml flask equipped with a CaCl₂ tube. After stirring for 30 min at room temperature, the solution was heated up to 70 °C for 5 min to remove methanol. After addition of some pellets of K₂CO₃, the remaining DMF solution was loaded directly onto a small silica column (Hex/Et₂O 9/1). Evaporation of the collected fractions under reduced pressure (*p* > 220 mbar) gave a colorless liquid (74 mg, 83%). ¹H NMR (CDCl₃, δ): 4.73–4.68 (m, 1H, H-3); 4.22 (quint, *J* = 6.1 Hz, 1H, H-2); 1.868 (d, *J* = 2.1 Hz, 3H, H-6); 1.80–1.35 (m, 10 H, *c*-hexylidene); 1.334 (d, *J* = 6.1, 3H, H-1). ¹³C NMR (CDCl₃, APT, δ): 109.6 (–, quaternary C of *c*-hexylidene); 83.7 (–, C-4); 75.2 (–, C-5); 73.5 (+, C-2); 69.6 (+, C-3); 37.7, 35.3, 25.1, 24.0, 23.8 (–, *c*-hex), 16.6 (+, C-1); 3.7 (+, C-6). IR (film, cm⁻¹): 2937, 2861, 2245 (C≡C). [α]_D²⁰ +10.3 (c 0.79 in CH₂Cl₂). HRMS: calcd for C₁₂H₁₈NaO₂ [M+Na]⁺ 217.1199, found 217.1206. The same procedure starting from diol **ent-7** resulted in product **ent-8**. [α]_D²⁰ –9.5 (c 0.69 in CH₂Cl₂).

5.1.7. Preparation of (4S,5S)-4,5-(cyclohexylidenedioxy)-hexan-2,3-dione (**9**) or **ent-9** 5S)-4,5-(cyclohexylidenedioxy)-hexan-2,3-dione (**9**) or **ent-9**

CCl₄ (0.7 ml), CH₃CN (0.7 ml) and a water solution containing NaIO₄ (151 mg, 0.70 mmol in 1.0 ml of H₂O) were added to a 6 ml vial containing acetal **8** (60 mg, 0.31 mmol). The mixture was stirred strongly and then RuO₂·H₂O (1.0 mg, 0.008 mmol, 0.025 equiv) was added. After 5 min (TLC Hex/Et₂O 1:1) the mixture was filtered through a compact layer of MPLC silica gel in CH₂Cl₂ (height 0.5 cm) covered by a layer of NaHCO₃ (height 0.5 cm). The filtrate was dried and evaporated under reduced pressure at 10 °C, affording a bright yellow oil which was immediately stored at –80 °C (32.3 mg, 46%). This material, which contained also unreacted **8** (19%), was not further purified to avoid loss of product due to the formation of hydrates on silica. ¹H NMR (CDCl₃, δ): 5.32 (d, *J* = 7.3 Hz, 1H, H-4); 4.65 (quint, *J* = 6.52 Hz; 1H, H-5); 2.36 (s, 3H, H-1); 1.90–1.20 (m, cyclohexylidene, superimposed on cyclohexanone), 1.11 (d, *J* = 6.52 Hz, 3H, H-6). The additional signals are due to the starting material (4.75–4.68 (m, 0.19H) ca. 19% mol) and cyclohexanone (br 2.35, 1.90–1.20). ¹³C NMR (CDCl₃, APT, δ): 198.0, 195.8 (–, C-2 and C-3); 110.8 (–, *c*-hex); 78.7 (+, C-4); 73.3 (+, C-5); 36.8, 34.8, 25.1, 24.02; 23.7 (–, *c*-hex.); 24.0 (+, C-1); 16.6 (+, C-6). IR (film, cm⁻¹) 2937; 2861; 1797 and 1714 (C=O); [α]_D²⁰ +16.0 (c 1.28, CH₂Cl₂). HRMS (DIP-EI-MS): calcd for C₁₂H₁₈O₄ 226.1205, found 226.1206. The same procedure starting from hex-**ent-8** gave **ent-9**. [α]_D²⁰ –14.4 (c 1.20; CH₂Cl₂).

5.1.8. Preparation of (2S,3S)-hex-4-yn-2,3-diol (**10**) or *ent*-**10**

CaCl₂·7H₂O (890 mg, 2.38 mmol, 1.2 equiv) was added to a stirred solution of ketone **6** (760 mg, 2.16 mmol) in MeOH (8 ml) under Ar. After the solid had dissolved completely (10 min) the solution was cooled to –50 °C, and NaBH₄ (122.6 mg, 3.24 mmol, 1.5 equiv) was added. After 10 min, a TLC control (Hex/EA 9/1) showed no starting material and H₂O (4 ml) was added carefully. Extraction of the white mixture with CH₂Cl₂ (3 × 5 ml), drying and evaporation of the organic phases gave a colourless, viscous liquid which contained semiprotected diol **16** and isomers with a migrated silylether group. ¹H NMR (CDCl₃, δ): 7.80–7.65 (m, 4H) and 7.50–7.30 (m, 6H); aromatics; 4.15–4.10 (m, 1H, C-3); 3.885 (quint. *J* = 6.0 Hz, C-2); 1.793 (d, 2.0 Hz, 3H, C-6); 1.09–1.06 (m, 12H, C-1 and C(CH₃)₃). This material was dissolved directly in THF (1 ml) under Ar and it was treated with a 1 M solution of TBAF in THF (2.11 ml, 2.11 mmol). After 5 h, the reaction was quenched with NH₄Cl (2 ml). After saturation of the water phase with solid NaCl, the mixture was exhaustively extracted with EA 5 × 5 ml. Purification by gravity on flash silica (Hex/EA 6/4) afforded a dense oil (131 mg, 53% over two steps). ¹H NMR (CDCl₃, δ): 4.09–4.03 (m, 1H, H-3); 3.75 (quint. *J* = 6.4 Hz, 1H, H-2); 2.48 (br, 2H, –OH); 1.867 (d, *J* = 2.1 Hz, 3H, H-6); 1.264 (d, *J* = 6.4 Hz, 3H, H-1). ¹³C (CDCl₃, APT, δ): 82.9 (–, C-4); 77.5 (–, C-5); 71.3 (+, C-2); 67.7 (+, C3); 18.4 (+, C-1); 3.56 (+, C-6). IR (film, cm^{–1}): br 3700–3000; 2976; 2923; 2237 (C≡C). Elemental analysis: found C 63.10, H 9.16; calc. for C₆H₁₀O₂ C 63.14, H 8.83%; *dr* = 0.95 (¹H NMR). The same procedure starting from *ent*-**6** gave *ent*-**10**; *dr* = 0.95 (¹H NMR).

5.1.9. Preparation of (2S,3S)-2,3-(cyclohexylidenedioxy)-hex-4-yne (**11**) or *ent*-**11**

The same procedure described above for acetal **8**, except for starting from diol **10** (110 mg, 0.96 mmol), resulted in acetal **11** (131 mg, 70%). ¹H NMR (CDCl₃, δ): 4.11 (dq, *J* = 8.15 Hz, *J* = 2.1 Hz, 1H, H-3); 4.00 (dq, *J* = 8.15 Hz, *J* = 6.1 Hz, 1H, H-2); 1.868 (d, *J* = 2.1 Hz, H-6); 1.80–1.35 (m, 10H, *c*-hexylidene); 1.17 (d, *J* = 6.1 Hz, H-1). ¹³C NMR (CDCl₃, APT, δ): 109.7 (–, *c*-hexylidene); 83.1 (–, C-4); 77.1 (+, C-2); 75.1 (–, C-5); 72.0 (+, C-3); 36.7, 36.0, 25.1, 23.8 (–, *c*-hexylidene); 16.9 (+, C-1); 3.8 (+, C-6). IR (film, cm^{–1}): 2937, 2862, 2245 (C≡C). HRMS (ESI-MS): calcd for C₁₂H₁₈NaO₂ [M+Na]⁺ 217.1199, found 217.1201. Applying the same procedure to diol *ent*-**10** gave acetal *ent*-**11**.

5.1.10. Preparation of (4R,5S)-4,5-(cyclohexylidenedioxy)-hexan-2,3-dione **12** or *ent*-**12**

Acetal **11** (103 mg, 0.53 mmol) was dissolved in CCl₄ (1.2 ml) and CH₃CN (1.2 ml) in a 6 ml vial. After adding a solution of NaIO₄ (258 mg, 1.21 mmol, 1.8 ml), Ru₂O·H₂O (1.8 mg, 0.013 mg, 0.025 equiv) was added and the mixture was stirred vigorously. After 5 min it was filtered directly over a compact layer of MPLC silica gel in CH₂Cl₂ covered with a layer of NaHCO₃ and eluted with CH₂Cl₂. Evaporation of the filtrate at reduced pressure at low temperature gave a yellow oil containing some starting material, which was purified on a small silica column (Hex/Et₂O 3/2). Evaporation at reduced pressure at 10 °C gave a bright yellow oil which was stored at –80 °C (41 mg, 34%). ¹H NMR (CDCl₃, δ): 4.59 (d, *J* = 7.25 Hz, 1H, H-4); 4.27 (dq, *J* = 7.25 Hz, *J* = 6.07 Hz, 1H, H-5); 2.38 (s, 3H, H-1); 2.0–1.5 (m, *c*-hexylidene, superimposed to cyclohexanone); 1.45 (d, *J* = 6.07 Hz, H-6). ¹³C NMR (CDCl₃, APT, δ): 198.8, 197.1 (–, C-2 and C-3); 111.8 (–, *c*-hexylidene); 82.7 (+, C-4); 74.2 (+, C-5); 37.0, 35.3, 25.0, 23.9; 23.7 (–, *c*-hexylidene); 24.9 (+, C-1); 19.0 (+, C-6); IR (film, cm^{–1}): 2937; 2864; 1797 and 1716 (C=O); HRMS (EI-MS): calcd for C₁₂H₁₈O₄ 226.1205, found 226.1207. The same procedure applied to acetal *ent*-**11** gave product *ent*-**12**.

5.1.11. General procedure for the preparation and characterization of 4,5-dihydroxyhexanediones (**4**)

A suspension of the corresponding dihydroxyhexanedione acetal (ca. 9.2 mg, 40 μM) in D₂O (3 ml) containing 1% of 1 M H₂SO₄ solution in H₂O was repeatedly sonicated using an ultrasound bath at 4 °C until the yellow color disappeared, due to the hydration of the α-diketone moiety. The solution was stirred in an ice bath, the hydrolysis was monitored by NMR and was complete after 18 h. The solution was extracted with 1/5 of the volume of CDCl₃ (600 μL) and the water phase was either used for biological assays or for NMR analysis. NOESY spectra were acquired with mixing time 300 msec. **Quantification.** An aliquot of the water phase (300 μL), acidic D₂O (276 μL) and a solution of Sodium Formate (200 mM, 24 μL, final concentration 8 mM) were transferred to a NMR tube and mixed. Quantitative ¹H NMR was recorded with the pulse program zgprde for the presaturation of H₂O (1%) and delay time of 30 s to allow full spin relaxation. The concentration of the DPD analog was calculated comparing the area of the formate peak with the sum of the doublet signals of H-4, and it was generally in the range of 6.5–8.5 mM in the mother solution, depending on the batch. **Derivatization with phenylenediamine.** The samples used for quantification were treated with 5 equiv of a 200 mM solution of Phenylenediamine hydrochloride in acidic D₂O, in the NMR tube and the solution was mixed. After 1 h ¹H NMR spectra were acquired.

5.1.12. Characterization of (4S,5S)-4,5-dihydroxyhexanedione ((4S,5S)-**4**) or (4R,5R)-**4**

¹H NMR (D₂O, δ): (**a**) 3.98 (quint. *J* = 6.4 Hz, 1H, H-5); 3.57 (d, *J* = 6.1 Hz, H-4); 1.400 (s, superimposed, H-1); 1.29 (d, *J* = 6.4 Hz, 3H, H-6); (**b**) 3.94 (d, *J* = 7.7 Hz, 1H, H-4); 3.78 (dq, *J* = 7.7 Hz; *J* = 6.4 Hz, 1H, H-5); 1.406 (s, superimposed on cyclohexanone, H-1); 1.31 (d, *J* = 6.4 Hz, 3H, H-6); **a:b** = 47:53. Additional signals in the spectrum were due to (2S,3R)-hex-4-yn-2,3-diol (**7**) derived from starting material **9** (region 4.3–4.2, 3.85–3.80 ppm; d, 1.8 ppm and d, 1.2 ppm) and acetic acid (s, 2.08 ppm). ¹³C NMR (D₂O, APT, δ), 102.0 (C-2) and 97.9 (C-3), **a** and **b**; **a**) 78.5 (+, C-4); 77.2 (+, C-5); 21.2 (+, C-1); 19.2 (+, C-6); **b**) 79.6 (+, C-4); 76.2 (+, C-5); 19.3 (+, C-1) 17.4 (+, C-6).

5.1.13. Characterization of (1R,2S)-1-(3-methylquinoxalin-2-yl)propane-1,2-diol ((1R,2S)-**17**)

¹H NMR (δ, ppm) 8.25–8.20 (m, superimposed to formic acid), 8.10–8.05 (m, 1H), 8.02–7.92 (m, 2H) aromatics; 5.15 (d, *J* = 6.6 Hz, 1H); 4.29 (quint. *J* = 6.5 Hz); 2.93 (s, 3H); 1.35 (d, *J* = 6.3 Hz, 3H). Other signals are due to (2S,3R)-hex-4-yn-2,3-diol (**8**). Of interest is the absence of the peaks due to the cyclic forms at 4.0–3.5 ppm, 1.41 and 1.40 ppm.

5.1.14. Characterization of (4R,5S)-4,5-dihydroxyhexanedione ((4R,5S)-**4**) or (4S,5R)-**4**

¹H NMR (D₂O, δ, ppm) **a**) 4.40 – 4.35 (m, 1H, H-5); 4.06 (d, *J* = 5.2 Hz, 1H, H-4); 1.42 (s, 3H, H-1); 1.15 (d, *J* = 6.7 Hz, 3H, H-6); **b**) 4.35 – 4.28 (m, 1H, H-5); 3.87 (d, *J* = 4.5 Hz, 1H, H-4); 1.36 (s, 3H, H-1); 1.25 (d, *J* = 6.7 Hz, H-6); **a:b** = 54:46. ¹³C NMR (D₂O, APT, δ, ppm) ¹³C NMR (APT, D₂O, δ): (**a**) 102.3 (C-2); 99.4 (C-3); 75.0 (+, C-4); 73.6 (+, C-5); 20.9 (+, C-1); 13.4 (+, C-6); **b**) 103.4 (C-2); 99.0 (C-3); 76.1 (+, C-5); 75.0 (+, C-4); 18.8 (+, C-1); 14.9 (+, C-6).

5.1.15. Characterization of (1S,2S)-1-(3-methylquinoxalin-2-yl)propane-1,2-diol ((1S,2S)-**17**)

¹H NMR: 8.10–8.06 (m, 1H); 7.98–7.94 (m, 1H); 7.88–7.80 (m, 2H); 5.14 (d, *J* = 5.0 Hz, 1H); 4.41–4.32 (m, 1H); 2.93 (s, 3H); 1.24 (d, *J* = 6.5 Hz, 3H). Of interest is the absence of the signals due to the cyclic forms: doublets at 4.06, 3.87, 1.15 and 1.25 ppm, as well as the singlets at 1.42 and 1.36 ppm.

5.2. Bioassays in *E. coli*

E. coli reporter strain KX1446 $\Delta LsrF$, $\Delta LsrG$ -, $\Delta luxS$ with *LacZ* fused to the *lsr* promoter was grown overnight in LB medium containing 100 mM MOPS buffer at pH 7. Stock solutions of the test compounds were diluted to a concentration of 2 mM with water containing H_2SO_4 0.01 M. As sample (4S,5S)-**4** had an impurity of diol **7**, a solution of **7** was also prepared in the same conditions and tested as control, and showed no activity in any of the assays. The following solutions/suspensions were transferred in test tubes in this order: LB medium (900 μ L), an aliquot of the overnight bacterial culture (10 μ M), acidic water and analog solution adding up to a volume of 100 μ L. Previous tests showed that the pH difference of the medium before (pH 6.62) and after (pH 6.35) addition of 10% volume of H_2SO_4 0.01 M was not significant, this was reflected by equal bacterial growth. For each series of measurement one control experiment with 100 μ L of H_2SO_4 0.01 M and one with Al-2 were carried out; each concentration was tested in three independent cultures. After 4.5 or 5 h cells were harvested, suspended in an equal volume of Z-buffer, and the optical density (OD₅₉₅) of each tube was recorded. The β -galactosidase activity of the protein extract was measured using *o*-nitrophenyl- β -D-galactopyranoside according to literature.³⁰ To observe the synergistic activity of the analogs, experiments were carried out in presence of 20 μ M DPD (**1**). The final concentration of the analogs was of 15 or 150 μ M. Diol **7** was tested at 50 μ M.

5.3. LuxP-FRET assay

In vitro response of LuxP-FRET protein was measured as described,³² optimized for 96 well plate reading using a multilabel counter (1420 Victor 3, Perkin Elmer).²⁵ Serial dilutions of test compounds were performed in water containing H_2SO_4 0.01 M and added to 12.5 μ g ml⁻¹ of CFP-LuxP-YFP chimeric protein in 25 mM of sodium phosphate buffer (pH 8), 35 mM NaCl, and 1 mM borate. Competition experiments were carried out in presence of 0.1 μ M DPD (**1**). Samples (2.5 μ l) were added to 280 μ l of reaction volume and FRET ratio was calculated (527/485 nm).

5.4. Bioluminescence assay in *V. harveyi*

V. harveyi in vivo response was measured using MM32 reporter strain grown in AB (autoinducer bioassay medium) as previously reported.¹¹ Serial dilutions were performed in water containing H_2SO_4 0.01 M. To determine light inhibition of analogs 0.1 μ M of DPD were added to cultures. Light emission was measured in a Wallac Model 1450 Microbeta scintillation counter after 5 h 30 min of incubation at 30 °C. Bioluminescence is reported as counts per minute (cpm) of the light emitted by the cultures. Half maximal effective concentration (EC₅₀) and half maximal inhibitory concentration (IC₅₀) were determined by fitting four parameter sigmoidal curves using non-linear least square analysis in a custom made Matlab program.

Acknowledgments

We thank Dr. Pedro Lamosa for his help in the discussion of NOESY results. The NMR spectrometers are part of the National NMR Network (REDE/1517/RMN/2005), supported by "Programa

Operacional Ciência e Inovação (POCI) 2010" and Fundação para a Ciência e a Tecnologia (FCT). F.R. acknowledges FCT and ITQB for funding. This work was supported by the FCT grants PTDC/QUI-BIQ/113880/2009 and PEst-OE/EQB/LA0004/2011.

Supplementary data

Supplementary data (NMR spectra of all new compounds, NOESY spectra of (4R,5S)-**4** and (4S,5S)-**4**) associated with this article can be found, in the online version, at doi:10.1016/j.bmc.2011.11.007.

References and notes

- Waters, C. M.; Bassler, B. L. *Annu. Rev. Cell Dev. Biol.* **2005**, *21*, 319.
- Xavier, K. B.; Bassler, B. L. *Nature* **2005**, *437*, 750.
- Bassler, B. L.; Wright, M.; Silverman, M. R. *Mol. Microbiol.* **1994**, *13*, 273.
- Lowery, C. A. *Chem. Soc. Rev.* **2008**, *37*, 1337.
- Federle, M. J. *Contributions to Microbiology*; Karger: Basel, 2009. Vol. 16, pp. 18–32.
- Zhu, J.; Miller, M. B.; Vance, R. E.; Dziejman, M.; Bassler, B. L.; Mekalanos, J. J. *PNAS* **2002**, *99*, 3129.
- Galloway, W. R. J. D.; Hodgkinson, J. T.; Bowden, S. D.; Welch, M.; Spring, D. R. *Chem. Rev.* **2011**, *111*, 28.
- Lowery, C. A.; Salzameda, N. T.; Sawada, D.; Kaufmann, G. F.; Janda, K. D. *J. Med. Chem.* **2010**, *53*, 7467.
- Semmelhack, M. F.; Campagna, S. R.; Federle, M. J.; Bassler, B. L. *Org. Lett.* **2005**, *7*, 569.
- Chen, X.; Schauder, S.; Potier, N.; Van Dorsselaer, A.; Pelczar, I.; Bassler, B. L.; Hughson, F. M. *Nature* **2002**, *415*, 545.
- Miller, S. T.; Xavier, K. B.; Campagna, S. R.; Taga, M. E.; Semmelhack, M. F.; Bassler, B. L.; Hughson, F. M. *Mol. Cell.* **2004**, *15*, 677.
- Pereira, C. S.; McAuley, J. R.; Taga, M. E.; Xavier, K. B.; Miller, S. T. *Mol. Microbiol.* **2008**, *70*, 1223.
- Pereira, C. S.; de Regt, A. K.; Brito, P. H.; Miller, S. T.; Xavier, K. B. *J. Bacteriol.* **2009**, *191*, 6975.
- Lowery, C. A.; Park, J.; Kaufmann, G. F.; Janda, K. D. *J. Am. Chem. Soc.* **2008**, *130*, 9200.
- Lowery, C. A.; Abe, T.; Park, J.; Eubanks, L. M.; Sawada, D.; Kaufmann, G. F.; Janda, K. D. *J. Am. Chem. Soc.* **2009**, *131*, 15584.
- Ganin, H.; Tang, X.; Meijler, M. M. *Bioorg. Med. Chem. Lett.* **2009**, *19*, 3941.
- Smith, J. A. I.; Wang, J. X.; Nguyen-Mau, S. M.; Lee, V.; Sintim, H. O. *Chem. Commun.* **2009**, 7033.
- Roy, V.; Smith, J. A. I.; Wang, J.; Stewart, J. E.; Bentley, W. E.; Sintim, H. O. *J. Am. Chem. Soc.* **2010**, *132*, 11141.
- Frezza, M.; Balestrino, D.; Soullère, L.; Reverchon, S.; Queneau, Y.; Forestier, C.; Doutheau, A. *Eur. J. Org. Chem.* **2006**, 4731.
- Peng, H.; Cheng, Y.; Ni, N.; Li, M.; Choudhary, G.; Chou, H. T.; Lu, C.-D.; Tai, P. C.; Wang, B. *ChemMedChem* **2009**, *4*, 1457.
- Defoirdt, T.; Miyamoto, C. M.; Wood, T. K.; Meighen, E. A.; Sorgeloos, P.; Verstraete, W.; Bossier, P. *Appl. Environ. Microbiol.* **2007**, *9*, 2486.
- Tsuchikama, K.; Lowery, C. A.; Janda, K. D. *J. Org. Chem.* **2011**, *76*, 6981.
- The PyMOL Molecular Graphics System, Version 1.4, Schrödinger, LLC.
- De Luca, L.; Giacomelli, G.; Taddei, M. *J. Org. Chem.* **2001**, *66*, 2534.
- Ascenso, O. S.; Marques, J. C.; Santos, A. R.; Xavier, K. B.; Rita Ventura, M.; Maycock, C. D. *Bioorg. Med. Chem.* **2011**, *19*, 1236.
- Kuethe, J. T.; Comins, D. L. *J. Org. Chem.* **2004**, *69*, 5219.
- Jung, M. E.; Piizzi, G. *Chem. Rev.* **2005**, *105*, 1735.
- Wheeler, O. H.; Rodriguez, E. E. G. D. *J. Org. Chem.* **1964**, *29*, 1227.
- Xavier, K. B.; Miller, S. T.; Lu, W. Y.; Kim, J. H.; Rabinowitz, J.; Pelczar, I.; Semmelhack, M. F.; Bassler, B. L. *ACS Chem. Biol.* **2007**, *2*, 128.
- Slauch, J. M.; Silhavy, T. J. *J. Bacteriol.* **1991**, *173*, 4039.
- Xavier, K. B.; Bassler, B. L. *J. Bacteriol.* **2005**, *187*, 238.
- Rajamani, S.; Zhu, J.; Pei, D.; Sayre, R. *Biochemistry* **2007**, *46*, 3990.
- Silverman, R. *The Organic Chemistry of Drug Design and Drug Action*; Elsevier Academic Press: Burlington, MA, USA, 2004. pp. 121–142.
- Lowery, C. A.; McKenzie, K. M.; Qi, L.; Meijler, M. M.; Janda, K. D. *Bioorg. Med. Chem. Lett.* **2005**, *15*, 2395.
- Motozaki, T.; Sawamura, K.; Suzuki, A.; Yoshida, K.; Ueki, T.; Ohara, A.; Munakata, R.; Takao, K.-I.; Tadano, K.-I. *Org. Lett.* **2005**, *7*, 2265.
- Xie, W.; Zou, B.; Pei, D.; Ma, D. *Org. Lett.* **2005**, *7*, 2775.